The Astrophysical Journal, 586:L61–L64, 2003 March 20

DISCOVERY OF X-RAY QUASI-PERIODIC OSCILLATIONS FROM AN ULTRALUMINOUS X-RAY SOURCE IN M82: EVIDENCE AGAINST BEAMING

Tod E. Strohmayer[1] and Richard F. Mushotzky[1]
Received 2003 January 3; accepted 2003 February 12; published 2003 February 25

ABSTRACT

We report the discovery with the European Photon Imaging Camera CCDs on board *XMM-Newton* of a 54 mHz quasi-periodic oscillation (QPO) in the greater than 2 keV X-ray flux from an ultraluminous X-ray source (ULX) in the starburst galaxy M82. This is the first detection of a QPO in the X-ray flux from an extragalactic ULX and confirms that the source is a compact object. On the basis of the QPO strength and previous *Chandra* observations, it appears likely that the QPO is associated with the most luminous object in the central region of M82, CXO M82 J095550.2+694047; however, *XMM* imaging alone is not sufficient to unambiguously confirm this. The other plausible candidate is CXO M82 J095551.1+694045; however, the QPO luminosity is comparable to the *peak* luminosity of this object in *Chandra* observations, which argues against it being the source of the QPO. The QPO had a centroid frequency of 54.3 ± 0.9 mHz, a coherence $Q \equiv \nu_0/\Delta\nu_{\rm fwhm} \approx 5$, and an amplitude (rms) in the 2–10 keV band of 8.5%. Below 0.2 Hz, the power spectrum can be fitted by a power law with index ≈1 and amplitude (rms) of 13.5%. The X-ray spectrum requires a curving continuum, with a disk blackbody at $T = 3.1$ keV providing an acceptable fit. A broad Fe line centered at 6.55 keV is required in all fits, but the equivalent width is sensitive to the continuum model. There is no evidence of a reflection component. The implied bolometric luminosity is $\approx(4–5) \times 10^{40}$ ergs s^{-1}. Archival *Rossi X-Ray Timing Explorer* pointings at M82 also show evidence for QPOs in the 50–100 mHz frequency range. We discuss the implications of our findings for models of ULXs.

Subject headings: black hole physics — galaxies: individual (M82) — galaxies: starburst — stars: oscillations — X-rays: galaxies — X-rays: stars

1. INTRODUCTION

Many galaxies harbor luminous, nonnuclear, pointlike X-ray sources. These ultraluminous X-ray sources (ULXs) can have apparent isotropic X-ray luminosities of 10–1000 times the Eddington limit for a neutron star. The presence of significant time variability on timescales of days to years argues for a compact accretor (see Ptak & Griffiths 1999) and has led to the suggestion that they may represent a new class of intermediate-mass black holes (IMBHs; Colbert & Mushotzky 1999; Makishima et al. 2000), perhaps formed as a result of binary interactions in dense stellar environments (see Portegies Zwart & McMillan 2002).

Current models for these objects center around two alternatives: (1) they are 50–1000 $M_\odot$ black holes radiating near the Eddington limit, or (2) they are "normal" (i.e., stellar mass) accreting binaries whose energy loss appears super-Eddington because it is beamed. These models are not without their difficulties. If they are IMBHs, standard accretion disk theory suggests that they should have lower disk temperatures than stellar mass black holes. Spectroscopy with *ASCA* (Makishima et al. 2000), however, does not support this conclusion unless they are rapidly rotating Kerr holes (see, however, Miller et al. 2003). Moreover, formation scenarios for IMBHs are challenging. Because of these difficulties, King et al. (2001) have argued for an association with standard X-ray binaries whose emission is beamed geometrically by factors of ∼10–100 (see also Zezas & Fabbiano 2002). Recently, Grimm, Gilfanov, & Sunyaev (2003) have demonstrated a connection between high-mass X-ray binaries (HMXBs) and star formation. This association supports the putative link between star formation and ULXs and suggests that they may reflect the high-mass end of the HMXB luminosity function. However, optical searches for the high-mass counterparts of the ULXs so far have not been very productive, and details of how sufficient beaming occurs at high-mass accretion rates are not well understood theoretically (Madau 1988; Kubota, Done, & Makishima 2002).

There is now extensive information on the timing properties of Galactic black hole candidates. In particular, the *Rossi X-Ray Timing Explorer* (*RXTE*) has discovered quasi-periodic oscillations (QPOs) with frequencies from 0.001 to 450 Hz (see Remillard et al. 2002). Many of these are correlated with spectral states. If ULXs are extragalactic analogs of the stellar mass binaries in our own galaxy, then they should show some of the same timing properties and spectral correlations. Although faint, the brightest sources are good candidates for low-frequency (∼1–100 mHz) QPO searches with large area imaging instruments, such as the European Photon Imaging Camera (EPIC) CCDs on board *XMM-Newton*.

One of the brightest ULXs is the source in M82 (CXO M82 J095550.2+694047, source 7 in Matsumoto et al. 2001, hereafter M82 X-1). Based on *ASCA* data, Ptak & Griffiths (1999) found both spectral and temporal variability in the hard X-ray flux from M82 and suggested it is from a compact object of ≈500 $M_\odot$. Recent *Chandra* High Resolution Camera (HRC) observations confirm that the ULX is not associated with the dynamical center of M82, nor is it associated with any radio active galactic nucleus (AGN) candidate or optically bright counterpart (Kaaret et al. 2001; Matsumoto et al. 2001). Here we report timing and spectroscopy of this object utilizing archival *XMM-Newton* and *RXTE* data.

2. *XMM* OBSERVATIONS AND DATA ANALYSIS

XMM-Newton observed M82 for 30 ks on 2001 May 5 at 09:19:40 (UT). For our study, we used only the EPIC data. We

[1] Laboratory for High Energy Astrophysics, Code 660, NASA Goddard Space Flight Center, Greenbelt, MD 20771; stroh@milkyway.gsfc.nasa.gov, richard@milkyway.gsfc.nasa.gov.

used the standard SAS version 5.3.3 tools to filter and extract images and event tables for both the PN and the MOS cameras. The PN and MOS images are dominated by a bright point source whose location is consistent with M82 X-1. At *XMM*'s spatial resolution, however, the field is crowded by several fainter sources resolved by *Chandra*. We have reexamined the available *Chandra* ACIS and HRC imaging, and we cannot rule out some contribution to the *XMM* flux from several nearby sources (sources 4, 5, and 6 in Matsumoto et al. 2001). Of these, sources 4 and 6 were not seen to vary with *Chandra* and were always *at least* a factor of ≈10 fainter than M82 X-1. Source 5 was found to be variable with *Chandra*, and at its brightest was a factor of 3.4 fainter than M82 X-1 at its faintest.

Chandra revealed diffuse emission in the central region of M82, which is also evident in the EPIC images and spectra. Inside an 18″ extraction radius, the emission from the diffuse thermal component is less than 10% of the point source at $E > 2$ keV; therefore, to increase the sensitivity to variability from the compact source, we use only the hard X-rays (>2 keV) for our timing study. We extracted events from the PN and MOS cameras within a 18″ circular region around the bright point source. To make the most sensitive search, we combined data from the PN and MOS cameras.

2.1. *Power Spectral Timing Analysis*

We calculated a power spectrum using a light curve sampled at $\frac{1}{2}$ s, yielding a 1 Hz Nyquist frequency. We used only the time interval for which both the PN and MOS were operating. This gave a continuous exposure of ≈27 ks. Figure 1 shows the 2–10 keV power spectrum rebinned by a factor of 128 in frequency space (with a frequency resolution of 4.7 mHz) for the PN+MOS (*bottom curve*), the PN only (*middle curve*), and the MOS only (sum of MOS1 and MOS2, *top curve*). There is a prominent QPO peak centered near 54 mHz in all three power spectra. We fitted the power spectrum using a model composed of a constant plus a power law and a Lorentzian. This model fits well, giving a minimum $\chi^2 = 185$ with 206 degrees of freedom (dof), and is shown in Figure 1 (*solid curve*). If the Lorentzian (QPO) component is excluded, χ^2 increases by ≈70. The significance of the QPO parameters can be estimated with the *F*-test and gives a probability of $\approx 3 \times 10^{-14}$, strongly indicating the need for the QPO component. As a second indication of the significance of the QPO, the single trial chance probability for the highest power in the QPO profile is 4.5×10^{-10}. On the basis of this and the *F*-test estimate, we are very confident in the QPO detection.

The 54 mHz QPO cannot be due to the PN sampling frequency of 73 ms. The sampling frequency and its aliases are not at or near the QPO frequency, and any aliased power from higher harmonics is greatly suppressed by the time binning. These instrumental features are also narrow, whereas the QPO is not. Similar arguments hold for the MOS analysis. We find no significant variability using $E < 2$ keV photons. This is consistent with the conclusion that much of the soft flux is from the diffuse emission and also provides additional evidence that the QPO is not an instrumental feature.

Our best power spectral model includes a power-law component, $A\nu^{-\alpha}$, with $\alpha = 1 \pm 0.12$, and an integrated variability (rms) of 13.5% from 0.1 mHz to 1 Hz. The QPO has a centroid frequency of 54.4 ± 0.9 mHz, a width $\Delta\nu_{\rm fwhm} = 11.4 \pm 2$ mHz, and an amplitude (rms) of 8.4% in the 2–10 keV band. We searched for energy and time dependence of the QPO amplitude but did not find any significant dependence.

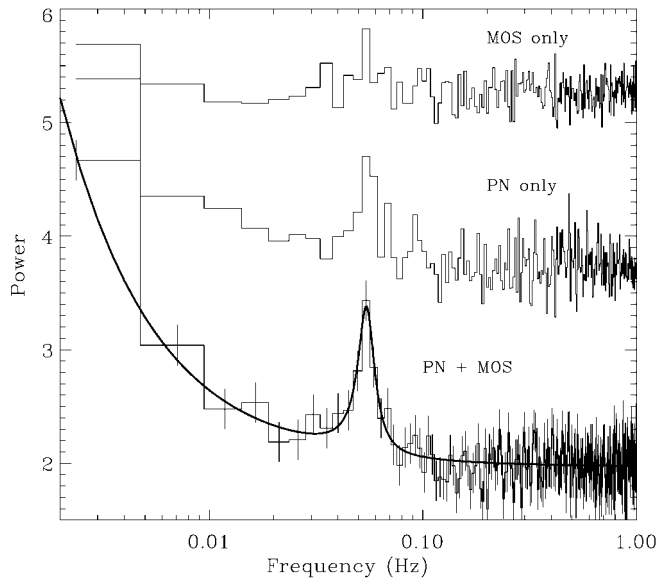

FIG. 1.—Power spectrum of the EPIC > 2 keV data from M82 X-1. The Nyquist frequency is 1 Hz. The frequency resolution is 4.7 mHz. The Poisson level has not been subtracted. Shown are the power spectra from the combined PN+MOS data (*bottom*), the PN only (*middle*), and the MOS only (*top*). The best-fitting power-law+Lorentzian model is shown as the thick solid curve (*bottom*).

2.2. *RXTE Timing Analysis*

Based on our *XMM* detection, we decided to search archival *RXTE* observations of M82 for similar timing features. Indeed, ∼100 ks of monitoring observations were carried out with *RXTE* from 1997 February to November (proposal 20203; see Rephaeli & Gruber 2002). These were typically 3–4 ks pointings utilizing three of the five Proportional Counter Array (PCA) detectors. We extracted light curves with a 128 Hz sampling rate using only the top xenon layer and events in the 2–20 keV energy band. Figure 2 shows power spectra from three observations with QPO detections. Each power spectrum is labeled with the corresponding observation ID. Model fits including a power law and a Lorentzian are also shown.

The most significant QPOs are in the 20203-02-04-00 and 20203-02-02-00 observations. These have frequencies of 107 ± 3 and 51 ± 2 mHz and *F*-test significances of 1.7×10^{-6} and 3.2×10^{-6}, respectively. To determine the QPO amplitudes, we first computed background count rates using the *RXTE*/PCA background models. This gave 2–20 keV source counting rates of ≈8–9 s^{-1} and corresponding amplitudes (rms) of about 9% for each QPO. The QPO frequencies, amplitudes, and coherences inferred from the *RXTE* data are similar to those derived from the *XMM* data. The flux levels inferred for the *RXTE* observations with QPOs are more or less consistent with the *XMM* flux level. The similar flux levels and QPO properties suggest that the source was in a similar state (see Rephaeli & Gruber 2002). *RXTE* monitoring also found a flux level higher by a factor of 3 on four occasions. Interestingly, these observations did not reveal any QPOs. Either the QPO source properties changed in a way suggestive of a correlation between spectral states and timing properties or perhaps an unrelated source or sources brightened and decreased the QPO sensitivity. With the *RXTE* data alone, it is not possible to decide between these alternatives.

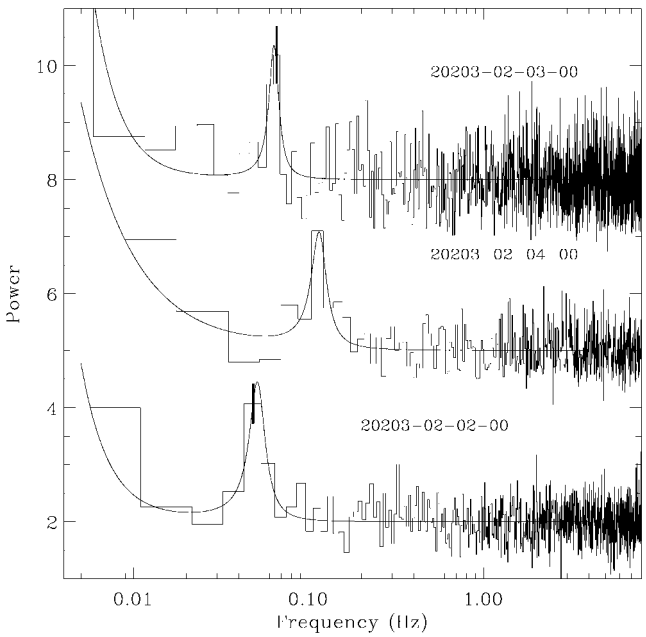

FIG. 2.—Power spectra from three *RXTE* observations of M82 that show low-frequency QPOs. Each spectrum is labeled with the corresponding observation ID. The best-fit models are also shown. For each spectrum, a typical error bar near the peak of the QPO feature is shown. The error bar for the middle curve (20203-02-04-00) has the same size as that shown for the bottom curve (20203-02-02-00).

2.3. *Energy Spectral Analysis*

We proceed under the assumption that a single source (most likely M82 X-1) dominates the *XMM* flux, but we comment below on the possible effects of source confusion. We obtained a spectrum by extracting an 18″ region around the bright source. This region has extensive diffuse emission that is spatially resolved by *Chandra* (see, for example, Kaaret et al. 2001). Fitting the *Chandra* ACIS spectrum of M82 X-1, one derives an effective column density of (0.5–0.9) × 10^{21} cm^{-2} depending on the continuum model used. We then fit the *XMM* data in the 3–10 keV band from all three instruments. We find that a power-law model is considerably worse than a disk blackbody (diskbb) or Comptonized (compst) model (minimum $\chi^2 =$ 2907 vs. 2385 or 2246, with 2021 dof), with the column density fixed to the range allowed by the *Chandra* data. There are broad residuals in the spectrum no matter what continuum model is used. These can be modeled by a variety of line shapes, including a relativistic broad line (the Laor model in XSPEC), the standard diskline model with extreme parameters ($q =$ -5.8 with the diskbb continuum), or a Gaussian. These fits indicate that much of the flux in the line comes from regions close to the black hole. The derived line parameters are sensitive to the continuum model used. The most "curved" continuum, the compst model, has the lowest EW (230 eV), while the power-law model (which fits poorly) has an EW of 1300 eV. There is no evidence for a reflection component. The line is centered at 6.55 ± 0.06 keV and has a Gaussian width of 0.33 (0.26–0.43) keV. Figure 3 shows the total spectrum of M82 inside the 18″ extraction radius.

The diskbb temperature, $T_{\rm in}$, is sensitive to the choice of column density; however, values less than 3 keV are strongly excluded. *Chandra* ACIS spectra of M82 X-1 that suffer no source confusion indicate $T_{\rm in} > 2.25$; however, the source was significantly fainter in these observations. There is a known positive correlation of $T_{\rm in}$ with luminosity for ULXs (Makishima et al. 2000), so that the higher temperature inferred from the *XMM* data is not inconsistent with the notion that the *XMM* spectrum is dominated by M82 X-1. The 2–10 keV flux is 2.1 × 10^{-11} ergs cm^{-2} s^{-1}. The bolometric flux of the compst model is 3.3 × 10^{-11} ergs cm^{-2} s^{-1}, while that of the diskbb model is 3.5 × 10^{-11} ergs cm^{-2} s^{-1}. Using a distance of 3.5 Mpc, this gives bolometric luminosities of ≈(4–5) × 10^{40} ergs s^{-1}. Assuming a similar spectrum and a single source, the bolometric luminosity of the object during the four brightest *RXTE* observations is 3 × larger or ∼1 × 10^{41} ergs s^{-1}.

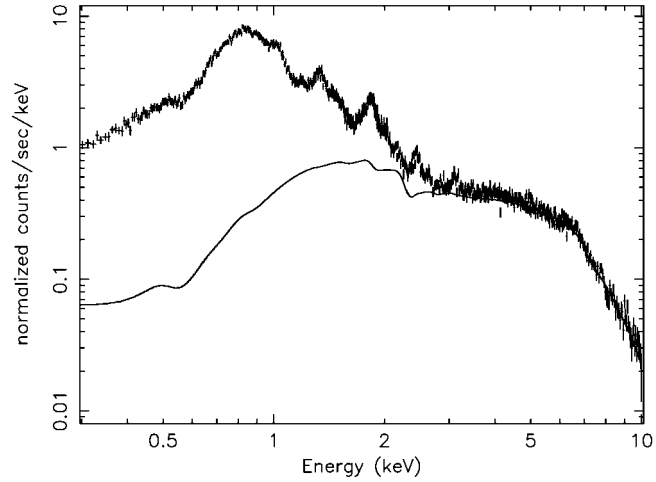

FIG. 3.—Count rate spectrum in the PN inside the 18″ extraction radius. The soft excess is from the diffuse thermal emission and was constrained based on *Chandra* observations that resolved the diffuse component. The emission above 2 keV is dominated by the point source.

3. DISCUSSION AND SUMMARY

What is the source of the QPO and Fe line? The effective temperature of the diffuse emission near M82 X-1 from the *Chandra* data is too low to produce an Fe K line. Moreover, it is unlikely that a diffuse process would produce a broad line. Unfortunately, the *Chandra* data for the point sources are not sensitive enough to detect the Fe K line seen in the *XMM* spectra. A number of arguments support the idea that M82 X-1 is the source of the QPO. (1) The *XMM* flux is consistent with the highest flux levels seen from M82 X-1 with *Chandra*. (2) The peak luminosity from *Chandra* observations of the other plausible candidate (source 5 in Matsumoto et al. 2001) was ≈3.5 × 10^{39} ergs cm^{-2} s^{-1}. This is comparable to the *luminosity* of the QPO, $L_{\rm QPO} \approx 0.085 \times 4 \times 10^{40} = 3.4 \times 10^{39}$ ergs cm^{-2} s^{-1}. So, either source 5 increased dramatically in brightness above what was seen in previous observations or it was modulated at ≈100% of its peak brightness to produce the QPO. These alternatives seem unlikely to us. A simpler interpretation is that both the QPO and the Fe line are produced in the same object, M82 X-1. However, it will likely require simultaneous *Chandra* and *XMM* observations to resolve this issue definitively.

The QPO discovery establishes beyond doubt the compact nature of the source. A firm upper limit to the size of the hard X-ray emission region is $r_{\rm source} < c/\nu_{\rm QPO} = 2.8 \times 10^6$ km $\approx 4\ R_\odot$. If the highest QPO frequency is associated with the Kepler frequency at the innermost circular orbit around a Schwarzschild black hole, then the mass must be $M_{\rm bh} < 1.87 \times 10^4\ M_\odot$.

Several Galactic microquasars, for example, GRS 1915+105,

GRO J1655−40, and XTE J1550−564, show low-frequency QPOs with similar frequency and strength as the QPOs described here (see Morgan, Remillard, & Greiner 1997; Remillard et al. 1999; Cui et al. 1999). For example, GRS 1915+105 shows ∼10–100 mHz QPOs at times when the source is in a "bright" state characterized by relatively modest broadband variability (10%–15% rms; see Morgan et al. 1997). To the extent that they can be compared, the timing properties of GRS 1915+105 in this state are similar to the properties of the M82 ULX reported here. The QPO frequencies, amplitudes, and coherences are similar, as is the broadband variability. The energy spectrum of GRS 1915+105 in such a state is also qualitatively similar to the inferred spectrum of M82 X-1, being fitted by a relatively hot diskbb.

These comparisons would seem to suggest that the M82 ULX may be an analog of the Galactic microquasars and thus that its mass is not extreme (see Greiner, Cuby, & McCaughrean 2001); however, there are difficulties with this conclusion. Detection of strong narrow QPOs provides evidence for the presence of a geometrically thin accretion flow (i.e., a disk; see van der Klis 1995; Di Matteo & Psaltis 1999), which argues against substantial beaming. For example, Madau (1988) has computed spectra from thick accretion disks that can have beaming factors approaching 25. The radiation field along the rotation axis is greatly enhanced by the multiple scattering of photons off the walls of the inner, luminous, funnel-shaped region. The funnel dominates the emission from tori viewed close to the symmetry axis. The presence of a narrow QPO challenges such a scenario for the M82 source, since multiple scatterings would degrade and broaden any QPO variability. Warped thin disks can also produce collimation (e.g., Pringle 1997; Maloney, Begelman, & Pringle 1996), and it is indeed predicted for objects near the Eddington limit; however, the amount of collimation/beaming is relatively modest and probably not sufficient to account for the factor of 50–100 required for M82 X-1. We note that the ≈7 hr periodic dipping/eclipsing modulation seen in a putative ULX in the Circinus galaxy (Bauer et al. 2001) also argues against substantial beaming in this source.

The broad Fe K line is also hard to understand in a beaming scenario, since this line is produced by the interaction of the X-ray continuum with cold material. In almost all beaming scenarios, the beam is emitted perpendicular to the axis of rotation (normal to the disk) and thus does not interact with high-density cold material. In addition, the ≈100 eV EW requires that a large covering factor of cold material be irradiated by the continuum. Finally, the analogy with extragalactic objects is clear; none of the known beamed sources (e.g., BL Lacertae objects) show Fe K lines, while a large fraction of the unbeamed objects (e.g., Seyfert galaxies) do.

Galactic black hole binaries also show ∼0.8–3 Hz "disk-corona" QPOs in the "very high" state (VHS; van der Klis 1995; Cui et al. 1999; Morgan et al. 1997). These QPOs are associated with a power-law spectral component (see Swank 2001) and a flat-topped noise that breaks to a steeper power law at about the QPO frequency (see Morgan et al. 1997 for examples from GRS 1915+105). Could the QPOs in M82 be the analog of these QPOs? If frequencies scale roughly as $1/M_{\rm bh}$, a mass of the order of 100–300 $M_\odot$ would be needed to obtain a 54–100 mHz QPO. However, the broadband variability in the M82 ULX and the lack of a nonthermal component argues against this identification.

We are left with something of a conundrum; the presence of strong narrow QPOs suggests that most of the flux in the 2–9 keV band originates from a disk, and thus the emission is not strongly beamed. However, no present disk models can produce a color temperature as high as seen in M82 X-1. The inferred inner disk radius using the diskbb model is ≈35 km (assuming that $T_{\rm in} = 3.1$ keV, a distance of 3.5 Mpc, an inclination angle of 45°, and no spectral hardening corrections). A Schwarzschild black hole of 4 $M_\odot$ would have a last stable orbit this size and further highlights the luminosity problem. This suggests that the diskbb model is probably unphysical; indeed, a Comptonization model seems more plausible. Since it now appears that the radiation is not strongly beamed, it is also difficult to explain the observed long-term bolometric luminosity with an object of less than 300 $M_\odot$, despite the apparent difficulties with such a scenario. The QPO frequency and the broad Fe K line are reminiscent of that seen in the Galactic microquasars in the VHS, but the continuum is rather different. We are thus left with the possibility that these objects show behavior not seen in any other black hole candidates, either in the Milky Way or as AGNs.

We thank Keith Arnaud, Craig Markwardt, and Jean Swank for many helpful discussions.

REFERENCES

Bauer, F. E., et al. 2001, AJ, 122, 182
Colbert, E. J. M., & Mushotzky, R. F. 1999, ApJ, 519, 89
Cui, W., Zhang, S. N., Chen, W., & Morgan, E. H. 1999, ApJ, 512, L43
Di Matteo, T., & Psaltis, D. 1999, ApJ, 526, L101
Greiner, J., Cuby, J. G., & McCaughrean, M. J. 2001, Nature, 414, 522
Grimm, H.-J., Gilfanov, M., & Sunyaev, R. 2003, MNRAS, in press (astro-ph/0205371)
Kaaret, P., et al. 2001, MNRAS, 321, L29
King, A. R., Davies, M. B., Ward, M. J., Fabbiano, G., & Elvis, M. 2001, ApJ, 552, L109
Kubota, A., Done, C., & Makishima, K. 2002, MNRAS, 337, L11
Madau, P. 1988, ApJ, 327, 116
Makishima, K., et al. 2000, ApJ, 535, 632
Maloney, P. R., Begelman, M. C., & Pringle, J. E. 1996, ApJ, 472, 582
Matsumoto, H., et al. 2001, ApJ, 547, L25
Miller, J. M., Fabbiano, G., Miller, M. C., & Fabian, A. C. 2003, ApJ, 585, L37
Morgan, E. H., Remillard, R. A., & Greiner, J. 1997, ApJ, 482, 993
Portegies Zwart, S. F., & McMillan, S. L. W. 2002, ApJ, 576, 899
Pringle, J. 1997, MNRAS, 292, 136
Ptak, A., & Griffiths, R. 1999, ApJ, 517, L85
Remillard, R. A., Morgan, E. H., McClintock, J. E., Bailyn, C. D., & Orosz, J. A. 1999, ApJ, 522, 397
Remillard, R. A., Muno, M. P., McClintock, J. E., & Orosz, J. A. 2002, in New Views on Microquasars, the Fourth Microquasar Workshop, ed. Ph. Durouchoux, Y. Fuchs, & J. Rodriguez (Kolkata: Center for Space Physics), 49
Rephaeli, Y., & Gruber, D. 2002, A&A, 389, 752
Swank, J. H. 2001, Ap&SS, 276, 201
van der Klis, M. 1995, in X-Ray Binaries, ed. W. H. G. Lewin, J. van Paradijs, & E. P. J. van den Heuvel (Cambridge: Cambridge Univ. Press), 252
Zezas, A., & Fabbiano, G. 2002, ApJ, 577, 726